[Resolution, focusing and counting rate]
(Chapter 6.2.8 of *Elements*)

Resolution, Focusing, and Counting Rate

The resolution of an eV spectrometer depends in part not only on the parameters of the detector, but also in part on the geometric arrangement of the components of the instrument, as illustrated in Figure 6-RFC-1. The geometric contributions to the time-of-flight resolution come about because the detailed flight path lengths and scattering angles depend on the point of emission from the source, the point of interaction in the sample, and the point of interaction in the detector. Meanwhile, the scattered neutron speed depends on the detailed angle of scattering, not simply the mean angle. The distances from the mean point on the surface of each component to the general points, s_m, s_s, and s_d, contribute linearly to the time of flight depends. The three are the independently distributed quantities whose contributions to the resolution variance add in quadrature. The detector final-energy resolution contribution is independent of these three, as is the incident-neutron emission-time distribution.

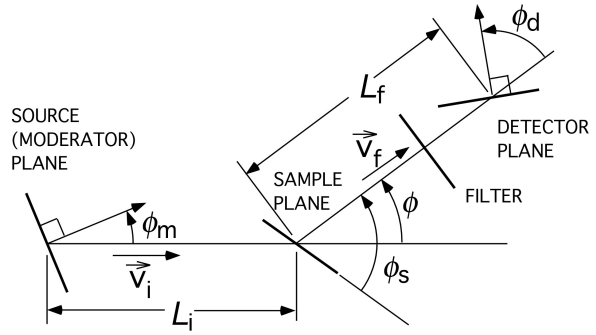

Figure 6-RFC-1 Schematic representation in the scattering plane of a general filter-detector type of eV spectrometer showing the definitions of focusable geometrical quantities. In a resonance-detector spectrometer the filter is a neutron capture-gamma converter that is a part of the detector and coincides with the detector plane.

Distances in the plane of the figure contribute to the resolution; contributions from out-of-plane distances are of higher order and can be ignored. Here we discuss some details of the resolution analysis. Independently distributed contributions to the energy transfer resolution come from the detector absorption probability discussed previously, and from the source size, sample size, and detector size, adding in quadrature.

It is an arduous exercise to develop expressions for the geometric contributions to the resolution, carried out in Carpenter, Watanabe, et al. (1983), which we spare the reader. The basis of the analysis is to compute times of flight for the small deviations of flight path lengths and scattering angles that follow from small deviations of general positions on the source, sample, and detector. The results for the standard deviations of the observed time-of-flight distribution follow. The geometric terms are all of the form

$$\sigma_i = a_i(\phi_i)\sin(\phi_i - \phi_i^o)\,\Delta S_i \Big/ \left(\sqrt{12}\,\mathrm{v}_f\right), \qquad \text{(6-RFC-1)}$$

where for each component $i = m,s,d$, the $a_i(\phi)$ are dimensionless factors that depend on the scattering angle, ϕ_i^o are *focusing angles* that depend in complicated ways on instrument parameters, ϕ_i are geometric angles as in Figure 6-RFC-1, ΔS_i are the full widths of the components measured across the scattering plane, and v_f is the nominal scattered-neutron speed.

When $\phi_i = \phi_i^o$ for all the components, geometric contributions to the resolution vanish and the instrument is completely focused, although intensity remains. Strictly, this can be done for only one detector position (scattering angle) because the moderator view and sample angle are common to all detectors. But awareness of the focusing conditions allows optimization of the resolution for an entire detector array. Similarly, the moderator-viewing angle may not be the instrument designer's to determine, and compromises are required.

The variance of the observed time-of-arrival distribution is

$$\sigma_t^{overall}(t)^2 = \sigma_t^{source}(E_i)^2 + \sigma_m{}^2 + \sigma_s{}^2 + \sigma_d{}^2 + \sigma_t^{abs}(E_f)^2, \qquad \text{(6-RFC-2)}$$

in which $\sigma_t^{source}(E_i)$ is the standard deviation of the source pulse emission time distribution at energy E_i (see *Elements* Chapter 2), and $\sigma_t^{abs}(E_f)$ is the standard deviation of the absorption time distribution, evaluated at the resonance energy (*Elements* Eq. 6.34).

Clock time is the measure of the duration of the measurement. The number of counts per unit clock time per unit time of arrival, $C(t)$, is

$$C(t) = I(E_i)\left|\frac{dE_i}{dt}\right|\frac{A_{sample}}{L_i^2}N_{sample}\frac{\partial^2\sigma}{\partial\Omega\,\partial E_f}(E_i,E_f,\phi)\frac{A_{\det}}{L_f^2}H(E_f). \qquad \text{(6-RFC-3)}$$

The time between the source pulse and the time of arrival at the detector is *t*. Here, $I(E_i)$ is the source angular current density at energy E_i, that is, the total number of neutrons emitted from the source surface per unit energy, per unit solid angle, per unit clock time, *n/eV-ster-s*. The Jacobian relating incident energy to time of arrival is $\left|\frac{dE_i}{dt}\right|$. From *Elements* (6.21) and (6.28),

$$\left|\frac{dE_i}{dt}\right| = \frac{2E_i v_i}{\left(L_i + L_f / f(\phi)\right)}. \qquad \text{(6-RFC-4)}$$

The area of the sample as viewed from the source is A_{sample}, and the number of scattering units in the sample is N_{sample}. The scattering cross section per scattering unit is $\frac{\partial^2\sigma}{\partial\Omega\,\partial E_f}(E_i,E_f,\phi)$ *barns/ster-eV*. The area of the detector as viewed from the sample is $A_{\det}$, and the efficiency-weighted integrated range of energies accepted by the resonance detector is $H(E_f)$. Calibration measurements using known reference scatterers establish the product of factors in Eq. (6-RFC-3) and other instrument parameters: scattering angles, flight path lengths, source intensity and emission time delay, and detector solid angle and efficiency, exclusive of the cross section to be measured. Usually used are uranium, lead, and vanadium metal. Mayers (1989), Fielding and Mayers (2002), and Mayers and Adams (2011) have described their calibration procedures for eV spectrometers.

The detector contribution to the intensity depends on the area under the absorption curves, which represents the product of the integrated detector efficiency and the width of the accepted energy band, so is expressed in units of energy. Figure 6-RFC-2 depicts the efficiency-area product of the scattered-neutron energy distribution, calculated for the Ta^{181} data of Fig. 6-RA-1. Although it is a convenient and conventional statistical measure of the width of a distribution, the second-moment integral expressing the variance does not converge for the absorption function. This is because the cross section is of Lorentzian form, and in the far wings the exponential tails approach that form, for which the second-moment integral diverges. Then, the straightforward FWHM measure is adequate (see Fig. 6-RFC-2).

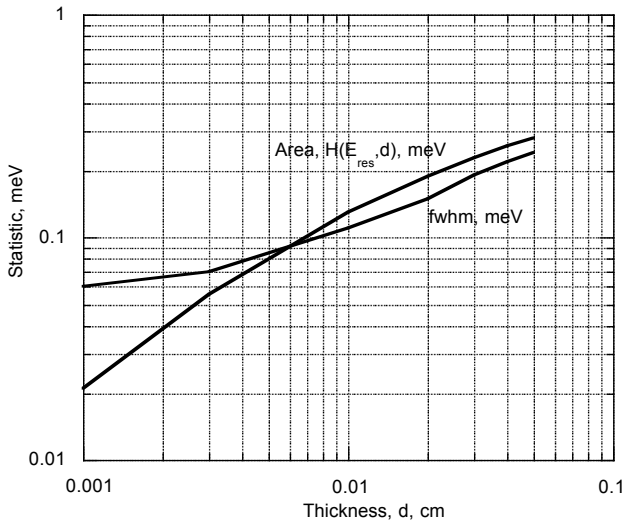

Figure 6-RFC-2. The area-efficiency product $H(E_{res},d)$ and the FWHM of the absorption probability for Ta^{181} foils of various thickness d.

Although the variance and standard deviation of the final-energy distribution may not exist, for purposes of resolution assessment, one may use the Gaussian-equivalent standard deviation of the energy-dependent absorption probability

$$\sigma_E^{abs} = \left(FWHM\right)_E^{abs} \Big/ \sqrt{8\ell n2}\,. \qquad \text{(6-RFC-5)}$$

The corresponding standard deviation of the time-of-flight distribution, σ_t^{abs}, resulting from the detector final energy distribution is

$$\sigma_t^{abs} = \left|\frac{\partial t}{\partial E_f}\right| \sigma_E^{abs}\,. \qquad \text{(6-RFC-6)}$$

In view of Eq. 6-RA-8 we can write

$$t = \frac{1}{v_f}(L_i f(\varphi) + L_f), \qquad \text{(6-RFC-7)}$$

so that

$$\sigma_t^{abs} = \frac{1}{2 v_f E_f}\left(L_i f(\varphi) + L_f\right)\sigma_E^{abs}. \qquad \text{(6-RFC-8)}$$

In *Elements* Chap. 8 (Detectors) we explore the physical arrangements of absorber foils and gamma-ray detectors in energy-sensitive detectors useful in eV spectrometers.

Instruments with closely packed gamma-ray detector arrays are subject to *cross talk*, in which photons from capture in absorbers associated with detectors at one angle see photons generated in absorbers associated with nearby angles. Such cross talk can be reduced by pulse-height discrimination, devised to reject the events from neighboring absorbers, although this reduces the desired counting rates. Because the distributions of photon flight path lengths differ for closely coupled absorber-detector assemblies from those for neighboring absorber-detector assemblies, one can speculate on the prospect of discrimination against cross talk using the resulting photon time-of-flight differences with anti-coincidence discrimination. Flight times are very short, sub-nanoseconds, but detectors and associated electronics may be fast enough to distinguish shapes of pulses from closely coupled absorber-detector assemblies from those for neighbor-absorber-detector assemblies, as well as their pulse amplitudes. Detectors in high-energy particle physics sometimes employ these methods.

Resonance prompt capture gamma spectra

In resonance capture gamma ray detector instruments, prompt capture gamma rays indicate neutron capture in the detector. These are emitted within ~ 10^{-15} seconds of the capture event, which is a negligible delay in practice. Typically, these appear in showers consisting of gamma ray emission from transitions between short-lived states of the capture-product nucleus, well resolved in energy. Users may refer to useful tables of energies and relative intensities of prompt capture gamma rays by Senftle, et al. (1971) for the low-energy capture gamma rays and intensities for thermal neutron capture, which are probably similar to those for resonance capture resonances. Another paper by Duffey et al. (1970) tabulates higher-energy (up to the binding energy of the captured neutron) capture gamma rays and intensities.

References

Senftle, F. E., H. D. Moore, D. B. Leep, A. El-Kady, and D. Duffey (1972). *Nucl. Instr. & Meth*. **93,** (p 425-459.
Duffey, D., El-Kady, and F. E. Senftle (1970), *Nucl. Instr. & Meth.* **80**, p 149-171.

Focusing

The resolution of an eV spectrometer depends in part not only on the parameters of the detector as in Fig. 6-RA-1, but also in part on the geometric arrangement of the components of the instrument, as illustrated in Fig. 6-RFC-1. The geometric contributions to the resolution come about because the detailed flight path lengths and scattering angles depend on the point of emission from the source, the point of interaction in the sample, and the point of interaction in the detector. The distances measured from the mean point on the surface of each component to the general points are s_m, s_s, and s_d, on which the time of flight depends linearly. The points on the three surfaces are the independently distributed quantities whose contributions to the resolution variance add in quadrature. The detector final-energy resolution contribution is independent of these three, as is the incident-neutron emission-time distribution.

Distances in the plane of the figure contribute to the resolution; out-of-plane distances are of higher order and can be ignored.

It is an arduous exercise to develop expressions for the geometric contributions to the resolution, carried out in Carpenter, Watanabe, et al. 1983, which we spare the reader. The basis of the analysis is to compute times of flight for the small deviations of flight path lengths and scattering angles that follow from small deviations of general positions on the source, sample, and detector.

The variance of the observed time-of-arrival distribution is

$$\sigma_t^{overall}(t)^2 = \sigma_t^{source}(E_i)^2 + \sigma_m^2 + \sigma_s^2 + \sigma_d^2 + \sigma_t^{abs}(E_f)^2, \qquad \text{(6-RFC-9)}$$

in which $\sigma_t^{source}(E_i)$ is the standard deviation of the source pulse emission time distribution at energy E_i (see *Elements* Chap. 2), and $\sigma_t^{abs}(E_f)$ is the standard deviation of the absorption time distribution, evaluated at the resonance energy, (6-RFC-6)). Equation 6-RFC-5 gives the incident energy E_i related to time *t* from the speed v_f, where the final energy is $E_f = E_{res}$. The standard deviations, (see *Elements* Eq. 6.20), of the geometric contributions to the time-of-arrival distribution, σ_m from the moderator σ_s from the sample, and σ_d from the detector, are all evaluated at speed v_f corresponding to $E_f = E_{res}$ consistent with (6-RFC-1) and depend on the angles φ_m, φ_s, and φ_d.

The results for the standard deviations of the observed time-of-flight distribution follow: for the moderator contribution,

$$\sigma_m = \frac{1}{v_f}\left|\frac{f(\phi)}{\cos\phi_m^o}\sin(\phi_m - \phi_m^o)\right|\frac{\Delta S_m}{\sqrt{12}}, \qquad \text{(6-RFC-10)}$$

where

$$\tan\phi_m^o = \frac{f(\varphi)\sin\varphi}{A - 1 + f(\varphi)\cos\varphi}. \qquad \text{(6-RFC-11)}$$

(Carpenter, Watanabe, et al. 1983)

For the detector contribution,

$$\sigma_d = \frac{1}{v_f}\left|\frac{f(\varphi)}{\cos\phi_d^o}\sin(\phi_d - \phi_d^o)\right|\frac{\Delta S_d}{\sqrt{12}}, \qquad \text{(6-RFC-12)}$$

where

$$\tan\phi_d^o = -\frac{L_i}{L_f}\tan\phi_m^o. \qquad \text{(6-RFC-13)}$$

For the sample contribution,

$$\sigma_s = \frac{1}{v_f}\left|\frac{f(\varphi)\sin\varphi}{\left(A-1+f(\varphi)\cos\varphi\right)}\frac{\left(A-1-f(\varphi)L_i/L_f\right)}{\cos\phi_s^o}\sin\left(\phi_s - \phi_s^o\right)\right|\frac{\Delta S_s}{\sqrt{12}}, \qquad \text{(6-RFC-14)}$$

where

$$\tan\phi_s^o = \frac{\left(A-2\right)\cos\varphi - \left(A-1\right)/f(\varphi) + f(\varphi)}{\sin\varphi\left(A-1-f(\varphi)L_i/L_f\right)}. \qquad \text{(6-RFC-15)}$$

Here, ΔS_m is the full width of the viewed source, measured on its surface intersection with the scattering plane. ΔS_s is the full width of the sample, and ΔS_d is the full width of the detector, all assumed to be uniform in intensity and sensitivity. (If these are not uniform the nonuniformity alters the factor $\sqrt{12}$.)

The geometric terms are all of the form

$$\sigma_i = a_i(\phi)\sin(\phi_i - \phi_i^o)\frac{\Delta S_i}{\sqrt{12}v_f}, \qquad \text{(6-RFC-16)}$$

where for each component $i = m,s,d$, the $a_i(\phi)$ are dimensionless factors that depend on the scattering angle, ϕ_i^o are *focusing angles* that depend on instrument parameters, ϕ_i are geometric angles as in Fig. 6-RFC-1, and ΔS_i are the full widths of the components measured across their intersection with the scattering plane, and v_f is the nominal scattered-neutron speed.

When $\frac{\partial\sigma_m^2}{\partial\varphi_m}=0$, $\frac{\partial\sigma_s^2}{\partial\varphi_s}=0$, and $\frac{\partial\sigma_d^2}{\partial\varphi_d}=0$, $\phi_m=\phi_m^o$, $\phi_d=\phi_d^o$, and $\phi_s=\phi_s^o$, the geometric contributions to the resolution vanish and the instrument is said to be completely geometrically focused. These conditions establish relationships among the geometric parameters of the instrument. This can be done for only one detector position (scattering angle) because the moderator view and sample angle are common to all detectors. But awareness of the focusing conditions allows optimization of the resolution for an entire detector array. Similarly, the moderator-viewing angle may not be the instrument designer's to determine, and compromises are required.

Counting Rate

Clock time is the measure of the duration of the measurement. The number of counts per unit clock time per unit time of arrival, $C(t)$, is

$$C(t)=I(E_i)\left|\frac{dE_i}{dt}\right|\frac{A_{sample}}{L_i^2}N_{sample}\frac{\partial^2\sigma}{\partial\Omega\partial E_f}(E_i,E_f,\varphi)\frac{A_{\det}}{L_f^2}H(E_f). \qquad \text{(6-RFC-17)}$$

The time between the source pulse and the time of arrival at the detector is t. Here, $I(E_i)$ is the angular current density at energy E_i, that is, the total number of neutrons emitted from the source surface per unit energy, per unit solid angle, per unit clock time, *n/eV-ster-s*. The Jacobian relating incident energy to time of arrival is $\frac{dE_i}{dt}$. From *Elements* Eqs. (6.21) and (6.28),

$$\left|\frac{dE_i}{dt}\right|=\frac{2E_iv_i}{\left(L_i+L_f/f(\varphi)\right)}. \qquad \text{(6-RFC-18)}$$

The area of the sample as viewed from the source is A_{sample}, and the number of scattering units in the sample is N_{sample}. The scattering cross section per scattering unit is $\frac{\partial^2\sigma}{\partial\Omega\partial E_f}(E_i,E_f,\varphi)$ *barns/ster-eV*. The area of the detector as viewed from the sample is $A_{\det}$, and the efficiency-weighted integrated range of energies accepted by the resonance detector is $H(E_f)$ (see Fig. 6-RFC-2). Calibration measurements using known reference scatterers (see *Elements* Chap. 7) establish the product of factors in Eq. (6-RFC-15) and other instrument parameters: scattering angles, flight path lengths, source intensity and emission time delay, detector solid angle and efficiency, exclusive of the cross section to be measured. Usually used are uranium, lead, and vanadium metal. Mayers (1989), Fielding and Mayers (2002), and Mayers and Adams (2011) have described their calibration procedures for eV spectrometers.

References

Carpenter, J. M., Watanabe, N., Ikeda, S., Masuda, Y., and Sato, S. (1983). A resonance detector spectrometer at KENS. *Physica*, **120 B**, 126.

Fielding, A. L. and J. Mayers (2002). "Calibration of the electron volt spectrometer, a deep inelastic scattering spectrometer at the ISIS pulsed neutron source" *Nucl. Instrum. Meth. A* **480**, 680-9.

Mayers, J. (1989). "Contributions of inelastic scattering to the vanadium differential scattering cross section; implications for the calibration of neutron spectrometers". *Nucl. Instrum. Meth. A* **281**, 654-6.

Mayers, J. and M. A. Adams (2011). "Calibration of an electron volt neutron spectrometer". *Nucl. Instrum. Meth. A* **625**, 47-56.